Analytical solution for filmwise condensation in the presence of noncondensables

Jia Liu[a], Roman O. Grigoriev[a]

[a]*School of Physics, Georgia Institute of Technology, Atlanta, GA 30332-0430, USA*

Abstract

This study revisits the problem of free vapor condensation in the filmwise regime by constructing and solving a comprehensive transport model that describes heat and mass transport through the gas phase, interfacial and thermal resistance of the condensate film, and heat conduction through the cooled wall in a self-consistent manner. We have shown that it is possible to obtain an analytical solution of the model which describes the net condensation fluxes in the presence of an arbitrary amount of noncondensables. This solution demonstrates that the overall thermal resistance reduces to a sum of the thermal resistances of the wall, the condensate film, the interfacial resistance, and the diffusive resistance of the gas layer only in the limit of infinite thermal resistance of the gas layer, but generally has a more complicated form. Finally, we derived an analytical solution for the condensate film thickness profile which generalizes Nusselt's classical laminar condensation solution. Both finite thermal conductivity of the wall and thermocapillary stresses were shown to play an important role, noticeably altering the thickness profile.

Keywords:

1. Introduction

Film condensation has been a widely studied topic due its relevance in many areas of technology. Fundamental understanding of vapor condensation is crucial in a wide variety of thermal management technologies that rely on phase change. A particularly important application is to heat exchangers, where vapor condensation on solid surfaces is often the limiting factor which controls heat transfer.

The first theoretical model of vapor condensation was developed by Nusselt [1] who assumed the thermal resistance is due entirely to the condensate film. Despite this and several other simplifications, Nusselt's theory has accurately predicted the heat transfer coefficient for condensation of pure vapor on highly conducting surfaces. As Othmer [2] discovered later, noncondensables have a large impact on condensation; the presence of as little as 0.5% of air in steam reduces the heat transfer coefficient by half. His results were later confirmed by a number of other studies [3, 4, 5, 6, 7] of steam condensation on vertical flat and cylindrical surfaces. The decrease in the heat transfer coefficient is due to the accumulation of noncondensable gas at the vapor-liquid interface, which forms a concentration boundary layer limiting the transport of vapor to the cold surface [8].

There is extensive literature devoted to this subject, with the bulk of theoretical studies focusing on condensation in the presence of forced convection. Forced flows tend to be turbulent, which makes the quantitative description of transport in the gas phase challenging. As a result, theoretical models tend to be rather arbitrary, with dependence on many important parameters expressed in terms of correlations based on empirical data rather than solid fundamental understanding of the problem. In order to make progress, the present study will instead focus on condensation in the presence of free convection.

Given that noncondensable gases tend to dissolve in liquids and are effectively impossible to remove completely, a comprehensive description of the condensation problem and the associated heat transfer has to involve at a minimum the following components. Transport of heat, momentum, and mass should be considered in the gas layer to account for the adverse effect of noncondensables. Transport of both heat and momentum should be considered in the liquid condensate film. Finally, heat transport needs to be considered in the solid wall to account for finite conductivity. The transport equations in the solid, liquid, and gas layer should be solved subject to the appropriate boundary conditions at the solid-liquid and liquid-vapor interface. To our knowledge, only a few studies [9, 10] have considered such a comprehensive and self-consistent model, but only numerical analysis has been performed.

Analytical (and even semi-analytical) results are extremely rare and involve considerable simplification of the problem. One of the most popular approaches known as the diffusion layer theory was introduced by Peterson and coworkers [11, 12] only considers transport in the liquid phase and the gas phase and leads to a rather simple, effectively one-dimensional description. The concentration and the temperature boundary layer are assumed logarithmic, which allows the heat flux to be expressed in terms of the condensation and sensible heat transfer coefficients. Both coefficients, however, are expressed in terms of correlations obtained by previous experimental studies [13], rather than computed from the transport equations. The condensate film is described using a standard lubrication-type model [14], but the corresponding heat transfer coefficient again involves correlations. Despite rather dramatic simplifications, no explicit solution for the heat transfer coefficient has been obtained, with the resulting system of equations that has

to be solved using an iterative procedure. Subsequent studies [15, 16, 6] used a similar approach.

A considerably more sophisticated and more rigorous theoretical description was proposed by Sparrow and Lin [17] who also considered transport inside the liquid layer and the gas layer. By seeking similarity solutions in both layers, this approach also makes the problem effectively one-dimensional, making it comparable to the diffusion layer theory in terms of complexity. However, the solutions are still constructed iteratively, so no explicit dependence on various parameters can be obtained. Moreover, the validity of this approach crucially relies on the assumption that the solution to the transport equations possess scaling that allows them to be expressed in similarity form. As we argue in the present paper, this assumption becomes invalid when thermocapillary stresses at the liquid-vapor interface are taken into account. Subsequent developments of this approach by Minkowycz and Sparrow [18], Rose [19], and Wu *et al.* [20] suffer from the same limitations.

While it is widely accepted that thermocapillary stresses play an important role in evaporation, e.g., leading to dry-out in heat pipes [21], oddly enough, the thermocapillary effect is almost universally ignored, without much justification, in considering filmwise condensation. As the present paper demonstrates, thermocapillary stresses arise inevitably in condensate films in response to variation in their thickness and can have a profound effect on the thickness profile and therefore the thermal resistance of the liquid layer. This is a good illustration of the kinds of limitations the lack of an explicit analytical solution describing film condensation can have: in the absence of an expression for the interfacial temperature it is difficult to judge the importance of a physical effect such as thermocapillarity.

The lack of an explicit relation between the heat transfer coefficient and the various material parameters and problem geometry is a significant limitation for our ability to improve thermal management technologies relying on phase change. Our study fills this void by formulating and solving a model describing transport in all three layers (solid/liquid/gas) and provides a clear physical insight into the problem of filmwise condensation in the entire range of the concentration of noncondensables. The focus on free filmwise condensation on a vertical plane allows us to obtain a tractable description that yields an explicit analytical expression for the heat transport coefficient which clearly identifies the physical effects that become the bottleneck in the heat transfer in various limiting cases. Our description also gives an explicit expression for the condensate film thickness profile and, in particular, shows that thermocapillary stresses make it more uniform compared with the boundary layer-type solutions of Nusselt [1] and Sparrow and Lin [17] that have become textbook examples.

The paper is organized as follows. Section 2 describes the mathematical model of the problem. The analysis of the model is presented in Section 3 and some applications in Section 4. Section 5 contains the summary and conclusions.

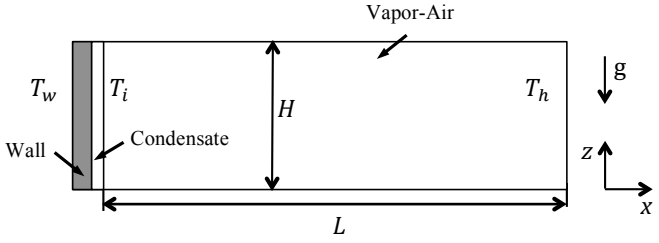

Figure 1: The geometry of the problem.

2. Mathematical model

The problem under consideration involves a mixture of vapor and air in a cavity of length L and height H in the presence of a horizontal temperature gradient. The hot vapor, which is assumed to be saturated on the right side of the cavity, condenses on a cooled vertical wall of thickness h_w on the left side of the cavity. The schematic illustration of the respective geometry is shown in Fig. 1. For simplicity we will consider a two-dimensional problem, where all physical observables depend only on the horizontal coordinate x and vertical coordinate z, but not the coordinate y, and the velocity field is planar, $\mathbf{u} = \hat{\mathbf{x}}u + \hat{\mathbf{z}}w$.

2.1. Governing equations

The heat and mass transport in the gas and the layer of liquid condensate are governed by the mass, momentum, and heat conservation equations

$$\nabla \cdot \mathbf{u}_\iota = 0, \tag{1}$$

$$\rho_\iota \left(\partial_t \mathbf{u}_\iota + \mathbf{u}_\iota \cdot \nabla \mathbf{u}_\iota\right) = -\nabla p_\iota + \mu_\iota \nabla^2 \mathbf{u}_\iota + \rho_\iota \mathbf{g}, \tag{2}$$

$$\partial_t T_\iota + \mathbf{u}_\iota \cdot \nabla T_\iota = \alpha_\iota \nabla^2 T_\iota, \tag{3}$$

where p and T are the pressure and temperature, respectively. The mass density ρ, thermal diffusivity α, and dynamic viscosity of the two fluids are considered constant. The index $\iota = g, l$ denotes the gas and the liquid phase, respectively. Finally, mass transport in the gas, which is a binary mixture of vapor and air, is governed by

$$\partial_t c_a + \mathbf{u}_\iota \cdot \nabla c_a = D \nabla^2 c_a. \tag{4}$$

where c_ι is the molar fraction of the two components of the gas phase, and D is the binary diffusion coefficient. To account for the finite thickness and conductivity of the solid walls, we will also use the heat equation

$$\partial_t T = \alpha_w \nabla^2 T_w, \tag{5}$$

where T_w is the temperature of the wall. Thermal diffusivities α_ι are related to thermal conductances k_ι via $k_\iota = \alpha_\iota \rho_\iota C_{p,\iota}$, where $C_{p,\iota}$ is the heat capacity of the gas/liquid/wall ($\iota = g, l, w$).

Since we are interested in the heat transport in steady state, we will set the temporal partial derivatives to zero in all of the above equations. In particular, the steady mass transport equation (4) in the gas can be rewritten in the form

$$\nabla \cdot \mathbf{j}_\iota = 0, \tag{6}$$

where

$$\mathbf{j}_\iota = n_g(\mathbf{u}_g c_\iota - D\nabla c_\iota) \tag{7}$$

is the number density flux of component i, $n_g = n_a + n_v$ is the net number density of the gas, and we have ignored the spatial variation in n associated with its dependence on the temperature, such that the molar fraction determines both the partial pressures and the number densities of the two components

$$c_\iota = \frac{p_\iota}{p_g} = \frac{n_\iota}{n_g}. \tag{8}$$

2.2. Boundary conditions

We will assume there is no heat or mass flux through the top and bottom of the cavity, and on the outer side $x = -h_w$ of the cooled wall the temperature is fixed

$$T_w = T_c, \tag{9}$$

e.g., due to the wall being in contact with a coolant at temperature T_c. We will also assume that at $x = L$ the gas has a fixed temperature

$$T_g = T_h \tag{10}$$

and the vapor is saturated. Such boundary conditions would describe a variety of practically relevant situations, e.g., the hot saturated vapor produced by evaporation of the liquid percolating through a porous wall of constant temperature T_h in the geometry shown in Fig. 1 or being injected from an external cavity along the centerline of a channel of width $2L$. The inner side $x = 0$ of the cooled wall is assumed to be covered by a thin layer of liquid condensate of thickness $h_l \ll h_w$. The heat flux balance at this interface requires

$$\mathbf{n} \cdot k_w \nabla T_w = \mathbf{n} \cdot k_l \nabla T_l, \tag{11}$$

where $\mathbf{n} = \hat{\mathbf{x}}$ is the surface normal. The heat flux balance at the liquid-vapor interface $x = h_l$ requires

$$\mathcal{L}J = \mathbf{n} \cdot k_g \nabla T_g - \mathbf{n} \cdot k_l \nabla T_l \tag{12}$$

where $\mathbf{n} = \hat{\mathbf{x}}$ again (assuming h_l is nearly uniform), $\mathcal{L}$ the latent heat of vaporization, and J is the mass flux associated with phase change (here condensation). The temperature at the liquid-solid and liquid-vapor interfaces is continuous

$$\begin{aligned} T_w &= T_l, \qquad x = 0, \\ T_l &= T_g, \qquad x = h_l. \end{aligned} \tag{13}$$

The mass/number conservation for the two components of the gas mixture at the liquid-vapor interface requires

$$\begin{aligned} \frac{J}{m_v} &= \mathbf{j}_v \cdot \mathbf{n} = n_g(\mathbf{n} \cdot \mathbf{u}_g c_v - D\mathbf{n} \cdot \nabla c_v), \\ 0 &= \mathbf{j}_a \cdot \mathbf{n} = n_g(\mathbf{n} \cdot \mathbf{u}_g c_a - D\mathbf{n} \cdot \nabla c_a), \end{aligned} \tag{14}$$

where m_v is the mass of one vapor molecule. Adding these we can find the normal components of the gas velocity

$$J = n_g m_v \mathbf{n} \cdot \mathbf{u}_g, \tag{15}$$

and the liquid velocity

$$J = \rho_l \mathbf{n} \cdot \mathbf{u}_l. \tag{16}$$

According to the kinetic theory of gases [22]

$$J = \beta u_t \rho_v \left[\frac{\sigma\kappa}{\rho_l R_v T_i} + \frac{\mathcal{L}}{R_v}\left(\frac{1}{T_s} - \frac{1}{T_i}\right)\right]. \tag{17}$$

Here R_v is the specific gas constant for the vapor, $u_t = \sqrt{R_v T_i}$ is the characteristic thermal velocity of the gas molecules, $\rho_v = m_v c_v n_g$ is the vapor concentration at the interface, σ is the surface tension, subscripts i and s denote values of the temperature at the interface and the saturation value for the vapor, respectively, and we have defined a shorthand

$$\beta = \sqrt{\frac{1}{2\pi}}\frac{\lambda}{2-\lambda}, \tag{18}$$

where λ is the accommodation coefficient (which can typically be set to unity). The first term in (17) can be neglected due to the negligible curvature κ of the liquid-vapor interface. The pressure dependence of the saturation temperature can be expressed using the Clausius-Clapeyron equation

$$\ln\frac{p_v}{p_v^0} = \frac{\mathcal{L}}{R_v}\left[\frac{1}{T_0} - \frac{1}{T_s}\right], \tag{19}$$

where p_v^0 is the saturation pressure at the reference temperature T_0, which we will set equal to T_h.

Finally, the stress balance at the liquid-vapor interface gives

$$(\Sigma_l - \Sigma_g) \cdot \mathbf{n} = \mathbf{n}(\kappa\sigma - J^2/\rho_g) - \gamma\nabla_s T_i \tag{20}$$

where $\Sigma = \mu[\nabla\mathbf{u} + (\nabla\mathbf{u})^T] - p$ is the stress tensor, $\nabla_s = (1 - \mathbf{n}\cdot\mathbf{n})\nabla$ is the surface gradient, the term J^2/ρ_g describes vapor recoil, $\gamma = -\partial\sigma/\partial T > 0$ is the temperature coefficient of surface tension, and the first term on the right-hand-side can be ignored. In addition, the tangential velocity components are continuous at $x = h_l$

$$(1 - \mathbf{n}\cdot\mathbf{n})(\mathbf{u}_l - \mathbf{u}_g) = 0 \tag{21}$$

and satisfy the no-slip boundary conditions at the solid-liquid interface

$$\mathbf{u}_l = 0. \tag{22}$$

Given that h_l is negligibly small compared with L, in the boundary conditions describing the liquid-vapor interface the quantities describing the gas phase can be evaluated at $x = 0$ instead of $x = h_l$.

3. Analysis

We will start our analysis by considering transport of heat, mass, and momentum in the gas layer, which tends to control the condensation rate and the associated heat transfer coefficient when the fraction of noncondensables exceeds a few percent. We will then consider the conjugate heat transfer problem

which involves the gas layer, the condensate film, and the cold wall, where spatial nonuniformity of the condensate film is neglected. Next, we will use the results for the condensation rate to derive a solution for the condensate film thickness that takes into account the gravitational draining as well as the thermocapillary stresses arising due to the nonuniformity of the film. Finally, we will validate the assumptions made in the analysis and illustrate how the results are affected by the concentration of noncondensables using a couple of specific examples.

3.1. Gas layer

It is natural to expect that convective flow in the gas layer could strongly modify the transport of heat and mass towards the cold wall, which would require the flow field be computed. However, this is not necessarily the case, at least for free convection in cavities with a high aspect ratio $\Gamma = L/H$. As numerical simulations reported in Ref. [23] illustrate, mass transport in the gas phase is often essentially one-dimensional even in the presence of convective flow. This can be understood via a simple calculation focusing on the central region of the cell. Let us introduce the nondimensional coordinates $\chi = x/H$ and $\zeta = z/H$, such that the interior of the cavity corresponds to $0 < \zeta < 1$ and $0 < \chi < \Gamma$. Since the flow field is constrained to the $\chi - \zeta$ plane and is incompressibile, it can be written in terms of the stream function $\psi(\chi, \zeta)$,

$$\mathbf{u}_g = \hat{\mathbf{x}} u_g + \hat{\mathbf{z}} w_g = \hat{\mathbf{x}} \partial_\zeta \psi - \hat{\mathbf{z}} \partial_\chi \psi. \tag{23}$$

In the limit of large Γ, the flow is essentially horizontal in the central region of the cavity with $u_g = O(\bar{u}_g)$ and $w_g = O(\Gamma^{-1}\bar{u}_g)$, where $\bar{u}_g$ is a characteristic flow velocity in the gas layer. We can therefore simplify (4) to read

$$H u_g \partial_\zeta c_v = D(\partial_\chi^2 c_v + \partial_\zeta^2 c_v), \tag{24}$$

with the vertical component u_z of the velocity yielding a higher order (in Γ^{-1}) correction. Furthermore, let $u_g = u_m + u_r$, where $u_m = \text{const} < 0$ is the mean component of the flow (the vapor flows towards the cold wall) and u_r describes the recirculation component with zero-mean

$$\int_0^1 u_r d\zeta = 0. \tag{25}$$

Correspondingly, we can write $\psi = u_m \zeta + \tilde{\psi}(\zeta) + O(\Gamma^{-1})$, where $u_r = \partial_\zeta \tilde{\psi}$, and

$$\int_0^1 \tilde{\psi}' d\zeta = \tilde{\psi}(1) - \tilde{\psi}(0) = 0. \tag{26}$$

In Ref. [23] the following solution to (24) was derived in the special case $u_r = 0$

$$c_v = C_0 + C_1 e^{-Pe_m \chi}, \tag{27}$$

where $Pe_m = |u_m| H/D$ is the Péclet number, which corresponds to the mean flow and the constants $C_0 > 0$ and $C_1 < 0$ are determined by the boundary conditions at $\chi = 0$ and $\chi = \Gamma$. In the general case (i.e., $u_r \neq 0$) the solution to (24) is

$$c_v = C_0 + C_1 e^{-Pe_m \chi}[1 + f(\zeta)], \tag{28}$$

where

$$f''(\zeta) = \frac{u_m u_r(\zeta) H^2}{D^2}[1 + f(\zeta)]. \tag{29}$$

The right-hand-side of (29), and hence $f(\zeta)$ itself, is of order $\epsilon = Pe_m Pe_r$, where $Pe_r = \max_z |u_r(z)| H/D$ is the Peclet number describing the strength of the recirculation flow u_r. Specifically,

$$f(\zeta) = \frac{u_m H^2}{D^2} \int \tilde{\psi}(\zeta) d\zeta + O(\epsilon^2). \tag{30}$$

Now, finally, the reason for separating u_x into the two components u_m and u_r becomes clear: the no-flux boundary condition for c_v requires $f'(0) = f'(1) = 0$ which is only consistent with (30) when (26) is satisfied. Note also that the characteristic velocity u_g for arbitrary $\bar{c}_a$ can be defined via the Peclet number $Pe_g = \bar{u}_g H/D = \max(Pe_m, Pe_r)$.

The crucial observation is that ϵ remains small regardless of the average concentration $\bar{c}_a$ of air: Pe_r becomes small in the limit $\bar{c}_a \to 0$, while Pe_m becomes small in the limit $\bar{c}_a \to 1$ [23]. Since ϵ is small, the z-dependence of the concentration field is weak and we can effectively treat it as a function of x alone. Since α_g and D are of similar magnitude for gases, the governing equations (3) and (4) are formally equivalent and so are the boundary conditions for c_v and T_g, the same arguments apply to the temperature field T_g, such that

$$T_g = B_0 + B_1 e^{-Pe_t \chi} + O(\epsilon), \tag{31}$$

where $Pe_t = |u_m| H/\alpha_g$ is the thermal Péclet number and B_0, B_1 are some constants. Since both c_v and T_g can be considered effectively z-independent and the condensate film is essentially flat, we can find solutions for $\mathbf{u}_g$, T_l, and T_w that are also effectively z-independent. The Navier-Stokes equation (2) and the incompressibility condition (1) admit the solution

$$\mathbf{u}_g = u_m \hat{\mathbf{x}}, \tag{32}$$

$$p_g = p_g^0 - \rho_g g z + O(\mu_g u_r / H^2) \approx p_g^0, \tag{33}$$

where

$$p_g^0 = \frac{p_v^0}{c_v|_{x=L}}. \tag{34}$$

The hydrostatic pressure term $\rho_g g z$ is negligible due to the low mass density of the gas and the viscous term $O(\mu_g u_r/H^2)$ is negligible due to the low velocity of the gas. Plugging (32) together with (27) into the boundary conditions (14) yields

$$\begin{aligned} c_a &= C e^{u_m x/D} = C e^{-rx/L}, \\ c_v &= 1 - C e^{u_m x/D} = 1 - C e^{-rx/L}, \end{aligned} \tag{35}$$

where we have defined a parameter

$$r = -\frac{u_m L}{D} = Pe_m \Gamma, \tag{36}$$

which represents nondimensional flux in the gas phase and

$$u_m = \frac{J}{m_v n_g} \tag{37}$$

according to (15). Note that both the diffusion constant

$$D = \frac{p_0}{p_g} D_0 \tag{38}$$

and the total number density

$$n_g = \frac{p_g}{m_v u_t^2} \tag{39}$$

depend on the average concentration of air $\bar{c}_a$ through p_g (cf. Eq. (34)). Here we set T_i equal to T_h in evaluating u_t, and D_0 and p_0 refer to the values of the diffusion coefficient and pressure at standard atmospheric conditions. However, since the product $n_g D$ is independent of p_g, the dimensional mass flux

$$J = -\frac{m_v n_g D}{L} r = -J_0 r \tag{40}$$

can only depend on $\bar{c}_a$ through r, where

$$J_0 = \frac{D_0 p_0}{L u_t^2}. \tag{41}$$

The coefficient C can be related to the average air concentration by integrating (35) over the cell

$$C = \frac{\bar{c}_a r}{1 - e^{-r}}. \tag{42}$$

Correspondingly, equations (3) and (5) governing heat transport in the liquid and the wall reduce to

$$\partial_x^2 T_l = \partial_x^2 T_w = 0 \tag{43}$$

with solutions

$$\begin{aligned} T_w &= T_c + B_2(x + h_w), \\ T_l &= T_i + B_3(x - h_l), \end{aligned} \tag{44}$$

with some constants B_2 and B_3. Using the boundary conditions (9)-(13) we obtain

$$T_g = T_h - B\left(e^{u_m x/\alpha_g} - e^{u_m L/\alpha_g}\right) = T_h - B\left(e^{-\eta r x/L} - e^{-\eta r}\right), \tag{45}$$

where $\eta = D/\alpha_g$ is the inverse of the Lewis number (which is independent of p_g and hence $\bar{c}_a$),

$$B = \frac{\Delta T - \mathcal{L} J_0 (Z_l + Z_w) r}{\eta r Z_g^{-1} (Z_l + Z_w) + 1 - e^{-\eta r}}, \tag{46}$$

where $Z_w = h_w/k_w$, $Z_l = \bar{h}_l/k_l$, and $Z_g = L/k_g$ are the well-known expressions for thermal resistivity of the cold wall, liquid condensate film, and the gas layer, respectively. The thickness h_l of the condensate film is nonuniform, hence Z_l is defined in terms of mean thickness $\bar{h}_l$.

3.2. Mass flux

According to (33)-(35) and (45), at the interface we have

$$\begin{aligned} T_i &= T_g|_{x=0} = T_h - B(1 - e^{-\eta r}), \\ \rho_v &= m_v n_g c_v|_{x=0} = \frac{1 - \bar{c}_a r - e^{-r}}{1 - e^{-r}} m_v n_g, \\ p_g &= \frac{p_v^0}{c_v|_{x=L}} = \frac{1 - e^{-r}}{1 - (1 + r\bar{c}_a) e^{-r}} p_v^0. \end{aligned} \tag{47}$$

Since $p_v = c_v p_g$, the saturation temperature T_s can be computed from (19) by evaluating the vapor concentration at the interface, yielding

$$\frac{1}{T_s} = \frac{1}{T_h} - \frac{R_v}{\mathcal{L}} \ln\left(\frac{c_v|_{x=0}}{c_v|_{x=L}}\right) = \frac{1}{T_h} - \frac{R_v}{\mathcal{L}} \ln\left(\frac{\bar{c}_a r + e^{-r} - 1}{\bar{c}_a r e^{-r} + e^{-r} - 1}\right). \tag{48}$$

Finally, the nondimensional flux r can be computed by substituting (40) and (48) into the KTG flux expression (17), which yields

$$\begin{aligned} r = -\frac{\beta \mathcal{L} u_t L}{R_v D} \frac{1 - \bar{c}_a r - e^{-r}}{1 - e^{-r}} \times \\ \times \left[\frac{1}{T_h} - \frac{1}{T_h - B(1 - e^{-\eta r})} - \frac{R_v}{\mathcal{L}} \ln\left(\frac{1 - \bar{c}_a r - e^{-r}}{1 - \bar{c}_a r e^{-r} - e^{-r}}\right)\right], \end{aligned} \tag{49}$$

where B and D depend on r and/or $\bar{c}_a$ according to (46) and (38).

An exact solution to the transcendental equation (49) cannot be obtained analytically. However, a reasonably accurate approximate solution can be obtained in explicit form by linearizing this equation about $r = 0$ and $\Delta T = 0$:

$$r = \Delta T \left[\frac{D_0 p_0 \mathcal{L} Z_2}{u_t^2 L} + \frac{D_0 p_0 T_h k_g u_t Z_3}{\beta \mathcal{L} L^2 p_v^0} + \frac{\bar{c}_a T_h k_g u_t^2 Z_3}{(1 - \bar{c}_a) \mathcal{L} L}\right]^{-1}, \tag{50}$$

where

$$Z_2 = Z_w + Z_l \tag{51}$$

is the thermal resistance of the wall and the liquid condensate and

$$Z_3 = Z_w + Z_l + Z_g \tag{52}$$

is the thermal resistance of the wall, liquid and gas layers. We can rewrite (50) in nondimensional form

$$r = \frac{u_t^2 L \Delta T}{D_0 p_0 \mathcal{L} Z}, \tag{53}$$

or, using (40), in dimensional form

$$J = -\frac{\Delta T}{\mathcal{L} Z}, \tag{54}$$

where the net thermal resistance

$$Z = Z_2 + \frac{Z_3}{Z_g}(Z_i + Z_d) \tag{55}$$

includes the contributions describing the interfacial resistance

$$Z_i = \frac{T_c u_t^3}{\beta \mathcal{L}^2 p_v^0} \tag{56}$$

and the diffusive resistance of the gas layer

$$Z_d = \frac{\bar{c}_a}{1-\bar{c}_a} \frac{L T_c u_t^4}{D_0 p_0 \mathcal{L}^2}. \tag{57}$$

This expression corresponds to the effective condensation thermal conductivity

$$k_c = \frac{1-\bar{c}_a}{\bar{c}_a} \frac{D_0 p_0 \mathcal{L}^2}{T_c u_t^4} = \frac{L}{Z_d} \tag{58}$$

derived by Peterson *et al.* [11].

It is worth emphasizing that, under the most general conditions, the net thermal resistance is not given by a simple sum of the resistances of the wall and liquid condensate $Z_2 = Z_w + Z_l$, interfacial resistance Z_i, and diffusive resistance Z_d, but also depends on the thermal resistance Z_g of gas layer. However, under typical conditions, due to both the large thickness of the gas layer and its poor thermal conductivity, Z_g will be many orders of magnitude larger than Z_l and Z_w for any $\bar{c}_a$, so that (55) can be simplified:

$$Z \approx Z_w + Z_l + Z_i + Z_d. \tag{59}$$

The corresponding net heat flux can be computed as

$$Q = -\mathcal{L} J + k_g \partial_x T_g|_{x=0}, \tag{60}$$

so that the corresponding heat transfer coefficient is given by

$$\mathcal{H} = \frac{Q}{\Delta T} = \frac{1}{Z_3} + \frac{Z_g}{Z_3}\frac{1}{Z}. \tag{61}$$

This heat transfer coefficient can be further simplified when $Z_3 \approx Z_g \gg Z$, in which case

$$\mathcal{H} \approx \frac{1}{Z}. \tag{62}$$

This result can also be derived from (54) and gives the expression for the heat transfer coefficient in a simple analytical form which (i) includes dependence on the problem geometry and material parameters and (ii) is easy to interpret. Specifically, we find that $\mathcal{H}$ is simplify the inverse of the net thermal resistance, which is a sum of four contributions: the resistance of the wall and the liquid condensate film, interfacial resistance, and the diffusive resistance of the gas layer.

3.3. Condensate film

Up until now we have assumed that the condensate film thickness h_l is small and nearly uniform; we need to check whether this is indeed the case. The flow inside this thin film can be described using lubrication approximation, where $\mathbf{u}_l = w_l(x)\hat{\mathbf{z}}$. In this approximation, the pressure in the liquid can be computed using (20)

$$p_l = p_g^0 - \rho_g g z - \sigma\kappa, \tag{63}$$

where the curvature of the interface is $\kappa = \partial_z^2 h_l$ in lubrication approximation and we have ignored the small vapor recoil pressure term. The vertical component of the Navier-Stokes equation (2) therefore reduces to

$$\mu_l \partial_x^2 w_l = \rho_l g + \partial_z p_l \approx \rho_l g - \sigma \partial_z^3 h_l, \tag{64}$$

since $\rho_l \gg \rho_v$. The solution satisfying the boundary conditions (20) and (22) is

$$w_l = \frac{\rho_l g - \sigma \partial_z^3 h_l}{2\mu_l}(x^2 - 2h_l x) - \frac{\gamma\tau}{\mu_l}x, \tag{65}$$

where $\tau = \partial_z T_i$ is the interfacial temperature gradient. Under our assumptions, the heat and mass flux are both independent of z, so that

$$Q \approx \frac{\Delta T}{Z} = k_l \frac{T_i - T_{wl}}{h_l}, \tag{66}$$

where T_{wl} is the temperature of the wall-liquid interface that is also independent of z. Hence,

$$\tau = \frac{\partial T_i}{\partial h_l}\partial_z h_l = \frac{\Delta T}{Z k_l}\partial_z h_l. \tag{67}$$

The corresponding volumetric flux is

$$q = \int_0^{h_l} w_l dx = \frac{\sigma h_l^3 \partial_z^3 h_l}{3\mu_l} - \frac{\rho_l g h_l^3}{3\mu_l} - \frac{\gamma \Delta T}{2\mu_l Z k_l} h_l^2 \partial_z h_l. \tag{68}$$

Mass conservation in the liquid together with the mass flux balance (16) requires that

$$\partial_z q = \frac{J}{\rho_l} \approx -\frac{\Delta T}{\rho_l \mathcal{L} Z}, \tag{69}$$

where $q = 0$ at the top of the cell $z = H$ (no flux through the top wall). Integrating this and substituting into (68) yields

$$-\frac{\sigma h_l^3 \partial_z^3 h_l}{3\mu_l} + \frac{\gamma \Delta T}{2\mu_l Z k_l} h_l^2 \partial_z h_l + \frac{\rho_l g h_l^3}{3\mu_l} = \frac{\Delta T}{\rho_l \mathcal{L} Z}(H - z). \tag{70}$$

The terms on the left-hand-side of this equation describe, respectively, the Young-Laplace pressure associated with the curvature of the interface, the thermocapillary stresses, and the gravitational draining, while the term on the right-hand-side describes the condensation mass flux.

The first term in (70) can be neglected if there are no high-curvature regions, such that the resulting differential equation can be rewritten as

$$\epsilon f' + f = 1 - \zeta, \tag{71}$$

where $f = (h/h_0)^3$, prime denotes the derivative with respect to $\zeta = z/H$,

$$\epsilon = \frac{\gamma \Delta T}{2 Z k_l H \rho_l g}, \tag{72}$$

is a (small) nondimensional parameter which determines the strength of thermocapillary stresses relative to gravity, and

$$h_0 = \left[\frac{3\mu_l H\Delta T}{\rho_l^2 g\mathcal{L}Z}\right]^{1/3} \tag{73}$$

is a characteristic thickness scale which describes the flux balance between condensation and draining due to gravity. Equation (71) can be solved analytically, yielding

$$h_l = h_0\left(1-\zeta+\epsilon\left[1-Ae^{-\zeta/\epsilon}\right]\right)^{1/3}, \tag{74}$$

where A is some constant. In fact, we should set $A = 0$ to ensure that the solution is well-behaved at $z = 0$ for $\epsilon \to 0$, which yields the following result for the mean thickness

$$\bar{h}_l = \frac{1}{H}\int_0^H h_l dz = \frac{3}{4}h_0\left[(1+\epsilon)^{4/3}-\epsilon^{4/3}\right]. \tag{75}$$

Note that, unlike Nusselt's classical laminar condensation result [1],

$$h_l = \left[\frac{4\mu_l k_l H\Delta T(1-\zeta)}{\rho_l^2 g\mathcal{L}}\right]^{1/4}, \tag{76}$$

in our model the thickness of the condensate film does not vanish at the top of the cold wall, where $h_l = h_0\epsilon^{1/3}$. This is the effect of thermocapillarity, which suppresses draining, making the condensate slightly thicker and more spatially uniform.

Finally, let us note that the curvature term that we dropped in (70) can be neglected when $|\partial_z^3 h_l| \ll \rho_l g/\sigma = \ell_c^{-2}$, where ℓ_c is the capillary length which is around 1 mm for most liquids. The highest curvature region of the condensate film corresponds to $z = H$, so we should have

$$\ell_c^2|\partial_z^3 h_l|_{z=H} = \frac{10h_0\ell_c^2}{27H^3}\epsilon^{-8/3} \ll 1, \tag{77}$$

This condition is only satisfied when thermocapillarity is sufficiently strong (ϵ is not too low). However, even when this condition is not satisfied, the resulting changes in the thickness profile near $z = H$ have negligible influence on the overall thermal resistance of the condensate layer.

4. Applications

To illustrate these results, we will discuss how they depend on the choice of the coolant fluid, the wall material, and the amount of noncondensable gases present in the cavity, which are among the most accessible design paramaters. Following a series of previous numerical [24, 25, 23], analytical [26], and experimental [27] studies, we will assume that a shallow layer of liquid coolant is confined inside a sealed rectangular cavity (cf. Fig. 2). An external temperature gradient is applied by maintaining the exterior surface of the cold wall at temperature T_c and the exterior of the hot wall at temperature $T_h = T_c + \Delta T$. As in a typical heat pipe, the liquid coolant evaporates at (or near) the hot wall, the vapor flows towards, and condenses, on the cold wall. To simplify things, we will avoid the discussion of evaporation and the temperature drop across the hot wall and simply assume that the hot wall is isothermal and the vapor is in thermal equilibrium with the liquid at $x = L$. We will assume that the geometry ($L = 48.5$ mm, $H = 10$ mm, $h_w = 1.25$ mm), reference temperature ($T_c = 293$ K), and the applied temperature differential ($\Delta T = 10$ K) are fixed at the values considered in the studies referenced above.

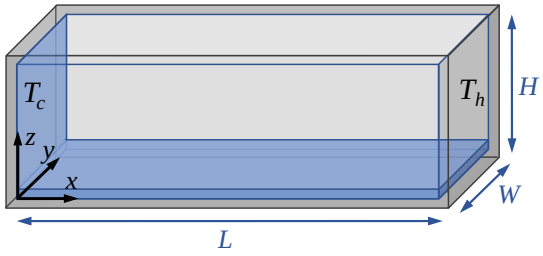

Figure 2: Test cell containing the liquid and air/vapor mixture. A layer of liquid (blue) is at the bottom of the cell and a thin film of condensate covers the entire cold wall. Thermal gradient in the x direction is imposed by maintaining the end walls at temperatures T_c and $T_h > T_c$.

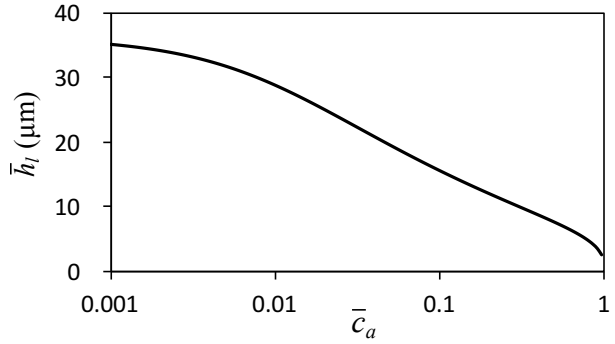

Figure 3: Dependence of the average thickness $\bar{h}_l$ of the condensate film on the air concentration $\bar{c}_a$ for condensation of silicone oil on fused quartz.

4.1. Silicone oil condensation on fused quartz

We will start by considering a volatile (0.65 cSt) silicone oil confined inside a test cell made of fused quartz (the values of all material parameters can be found in Ref. [23]). All of our calculations were restricted to a range of $\bar{c}_a$ varying from a minimum of 0.001 (i.e., 0.1% air), which in all likelihood is well below the value that can be achieved in practice, to the maximum $1 - p_v^0/p_0$ (i.e. 96% air), which corresponds to the atmospheric pressure p_0, when the gas predominantly contains air.

In order to obtain solutions, exact or approximate, of the model we first substitute (59), (72), and (73) into (75) and solve the resulting equation for the the mean thickness of the condensate film $\bar{h}_l$ for a fixed $\bar{c}_a$. The results for different $\bar{c}_a$ are plotted in Fig. 3, which shows that $\bar{h}_l$ varies from the maximum of around 35 μm when there is essentially no air inside the cell to around 2.6 μm at ambient conditions, when the gas is predominantly air with only 4% vapor. The thickness profile $h_l(z)$ for the lowest value of the air concentration $\bar{c}_a = 0.001$ is shown in Fig. 4. The thickness of the film varies between 15 μm at the top of the cold wall ($\zeta = 1$) to 46 μm at the bottom ($\zeta = 0$).

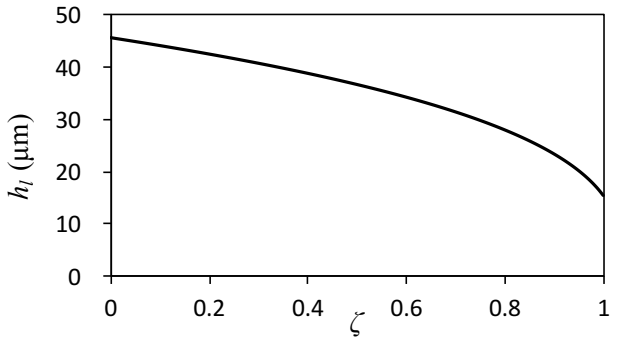

Figure 4: Thickness profile $h_l(\zeta)$ of the silicone oil condensate film for $\bar{c}_a$ = 0.001.

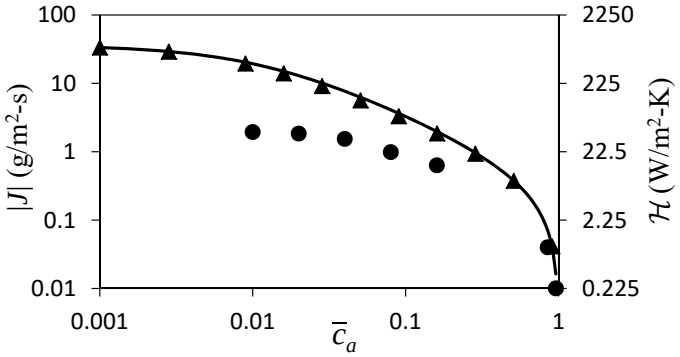

Figure 5: Dependence of the mass flux J and heat transfer coefficient $\mathcal{H}$ on the air concentration $\bar{c}_a$ for condensation of silicone oil on fused quartz. Exact numerical solution is shown as a solid curve, the approximate analytical solution as triangles, and the numerical result from Ref. [23] as circles.

Once the thickness of the condensate film has been determined, its thermal resistance can be found, which allows computation of the mass and heat flux associated with the condensation process. The condensation mass flux J (or rather its absolute value, since $J < 0$) and the corresponding heat transfer coefficient $\mathcal{H}$ are shown in Figure 5. The approximate analytical solution based on equation (50) is found to be virtually indistinguishable from the exact numerical solution of equation (49) in the entire range of composition of the gas phase, which attests to the excellent accuracy of the approximation. The figure also compares these results with the numerical ones obtained in a previous study [23] which assumed that the walls of the container are partially wetting, so that condensation occurs exclusively at the surface of the liquid layer which covers the bottom of the cell (cf. Fig. 2). Not surprisingly, the condensation mass flux (and therefore the heat transfer coefficient) is substantially higher when the vapor condenses on the cold wall instead. The difference can be as large as an order of magnitude at low values of $\bar{c}_a$ under otherwise identical conditions and reflects both the larger area over which the condensation occurs and the smaller thermal resistance of the thin film of condensate covering the cold wall.

In conclusion of this section, let us compare the relative magnitude of different contributions to the overall thermal resistance Z of the whole system. The four contributions (Z_d, Z_i, Z_l, and Z_w) are plotted as a function of the average concentration of air $\bar{c}_a$ in Fig. 6. Not surprisingly, at high $\bar{c}_a$ when mass transport is severely suppressed by diffusion through air, thermal resistance is dominated by the diffusive contribution. In fact Z_d remains the largest contribution for when the gas contains as little as 1% of air. At even smaller air concentrations, the thermal resistance of the wall becomes the dominant contribution, which is also not surprising given that the walls are relatively thick and fused quartz is a relatively poor conductor. The thermal resistance of the liquid and the interfacial resistance are negligible in this particular scenario, but may become important when the walls material has high thermal conductivity, as illustrated below.

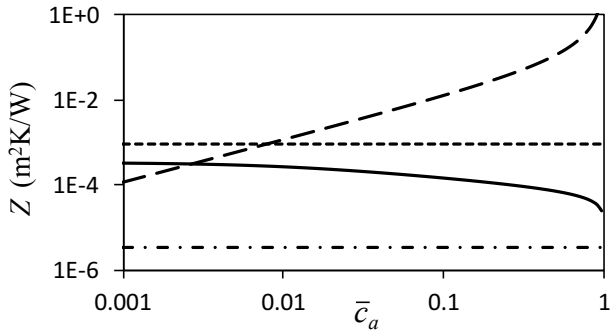

Figure 6: Thermal resistance of the liquid (Z_l, solid line), the wall (Z_w, short-dash line), the interfacial resistance (Z_i, dash-dot line), and the diffusive resistance of the gas layer (Z_d, long-dash line) for silicone oil condensation on fused quartz at various air concentration.

4.2. Water condensation on copper

A more practical application of our study is towards characterizing heat transfer in heat pipes and heat spreaders, which commonly use water as the coolant inside sealed copper containers. Hence, we will next consider water confined inside a test cell made of copper, but with the geometry (length, height of the cavity, wall thickness) that is the same as that considered in the previous section to enable direct comparison.

The average thickness $\bar{h}_l$ of the condensate film is plotted as a function of $\bar{c}_a$ in Fig. 7. It varies from the maximum of around 44 μm at $\bar{c}_a = 0.001$ to around 2 μm at ambient conditions, when the gas mixture contains just over 2% of water vapor. This is very similar to the results we have obtained for silicone oil, since for the water/copper combination the higher latent heat is offset by the lower overall thermal resistance in the denominator of (73). The thickness profile $h_l(z)$ for the lowest value of the air concentration $\bar{c}_a = 0.001$ is shown in Fig. 8. The thickness of the condensate film varies between 27 μm at the top of the cold wall ($\zeta = 1$) to 54 μm at the bottom ($\zeta = 0$), also similar to the result of the previous section.

The corresponding condensation mass flux J and heat transfer coefficient $\mathcal{H}$ are shown in Figure 9. Again we find the approximate analytical solution based on equation (50) to be in excellent agreement with the exact numerical solution of equation (49) in the entire range of composition of the gas phase. The condensation mass flux is comparable to that for the silicone oil/fused quartz case (as in the case of condensate film thickness, this is because for the water/copper combination the

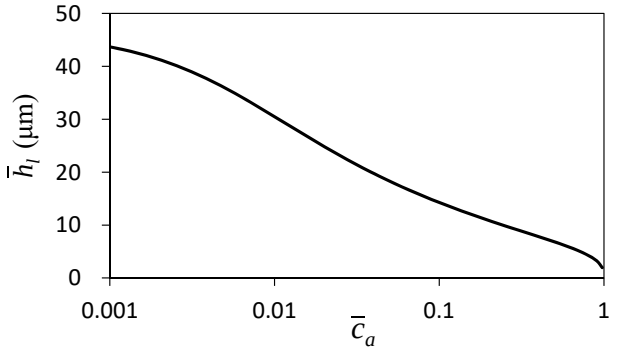

Figure 7: Dependence of the average thickness $\bar{h}_l$ of the condensate film on the air concentration $\bar{c}_a$ for condensation of water on copper.

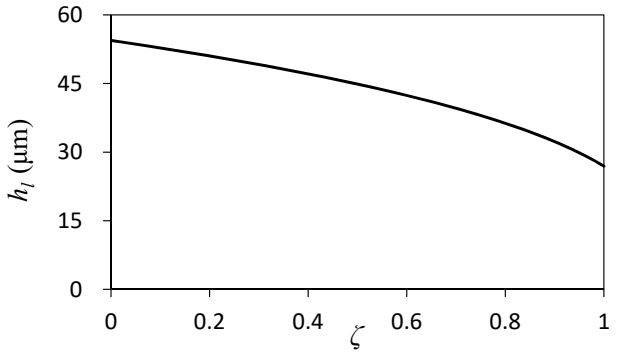

Figure 8: Thickness profile $h_l(\zeta)$ of the water condensate film for $\bar{c}_a = 0.001$.

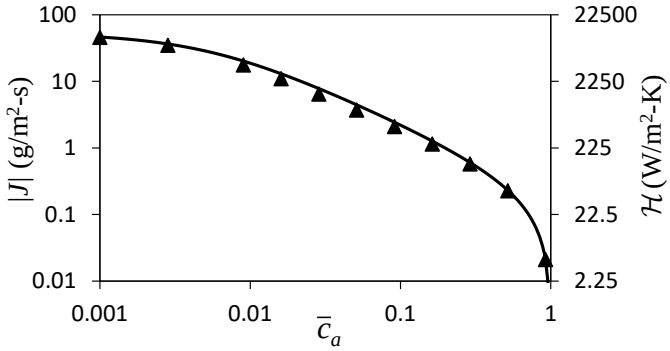

Figure 9: Dependence of the mass flux J and heat transfer coefficient $\mathcal{H}$ on the air concentration $\bar{c}_a$ for condensation of water on copper. Exact numerical solution is shown as a solid curve and the approximate analytical solution as triangles.

higher latent heat is offset by the lower overall thermal resistance in the denominator of (69)). In contrast, the heat transfer coefficient is substantially higher for the water/copper combination: for $\bar{c}_a = 0.001$ we find $\mathcal{H} \approx 10^4$ W/(m^{2}K) compared with $\mathcal{H} \approx 750$ W/(m^{2}K) for the silicone oil/fused quartz combination, illustrating the clear advantage of water (due to its high latent heat) and copper (due to its high thermal conductivity).

The relative magnitude of different contributions to the overall thermal resistance Z as a function of the average concentration of air $\bar{c}_a$ are shown in Fig. 6. We find that thermal resistance is dominated by the diffusive contribution over almost the entire range of $\bar{c}_a$. Thermal resistance of the condensate film be-

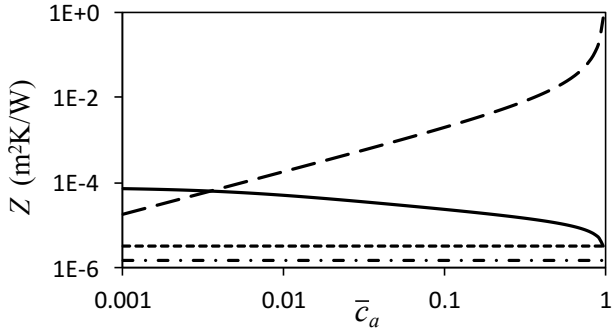

Figure 10: Thermal resistance of the liquid (Z_l, solid line), the wall (Z_w, short-dash line), the interfacial resistance (Z_i, dash-dot line), and the diffusive resistance of the gas layer (Z_d, long-dash line) for water condensation on copper at various air concentration.

comes the dominant contribution only at extremely low $\bar{c}_a$ when the gas contains merely 0.3% of air, which in all likelihood is impossible to achieve in practice since air tends to dissolve well in water. Thermal resistance of the wall is negligible because copper is a very good thermal conductor. Similarly, the interfacial resistance (56) is negligibly small, again due to the high latent heat of water.

As the two examples considered here illustrate, the thermal resistance of the condensate film becomes the dominant factor limiting heat and mass flux only under rather extreme conditions (when noncondensables have been effectively completely removed) that may never be realized in practice. It is only in this case that the one-dimensional approximation for the heat and mass transport in the gas phase may become invalid. However, even in this limit our model should produce reasonably accurate predictions for the net heat and mass flux. Note that the condensate film thickness profile in this limit (cf. Figs. 4 and 8) remains relatively uniform, unlike the Nusselt's solution which predicts that the condensate film thickness vanishes at the top of the cold wall, resulting in a divergence of the heat and mass flux there. This is the only component of the entire problem that breaks the symmetry of the solution in the vertical direction. Our results predict no divergence, with the film thickness h_l and therefore its local thermal resistance h_l/k_l varying relatively little about the mean. As a result, heat and mass flux in the gas layer, especially at high aspect ratio Γ can be still be considered effectively one-dimensional.

Finally, let us comment on the effect of geometry on the condensate film thickness. As equations (73) and (75) illustrate, $\bar{h}_l \propto H^{1/3}$ scales rather weakly with the height of the container for all $\bar{c}_a$. The dependence on the thickness L of the gas layer is due primarily to the diffusive resistance (57), which becomes dominant at typical conditions when the gas contains more than about 0.3% air, when $\bar{h}_l \propto (H/L)^{1/3}$. Consider, for instance, condensation of saturated steam on a 1 m-tall wall of a heat exchanger, with the characteristic thickness of the gas layer being 1 cm, in the presence of 1% of air. In this configuration we will have $\bar{h}_l = 130$ μm, compared $\bar{h}_l = 30$ μm for $H = 1$ cm and $L = 4.85$ cm at the same $\bar{c}_a$.

5. Conclusions

In this paper we have introduced and solved a comprehensive physical model of filmwise vapor condensation under the assumption of free convection. Unlike common engineering models that take a piecemeal approach and treat only a few aspects of the problem, our approach describes all aspects of condensation, including heat and mass transport through the gas phase, interfacial and thermal resistance of the condensate film, and heat conduction through the cooled wall in a self-consistent manner. We have shown that heat and mass transport in the gas layer can be considered one-dimensional under rather general conditions, even when there is convective flow present. Most importantly, we have obtained an approximate analytical solution which shows excellent agreement with the exact numerical solution of the model in the presence of an arbitrary amount of noncondensable gases such as air.

The analytical solution for the condensation mass flux (and the corresponding heat flux) allows an easy interpretation, with explicit dependence on all of the parameters of the problem. For example, the overall thermal resistance is found to be given by a sum of the thermal resistances of the wall, the condensate film, the interfacial resistance, and the diffusive resistance of the gas layer – all given by the familiar standard expressions – in the limit of infinite thermal resistance of the gas layer. It is important to note, however, that this simple additive relation breaks down when the thermal resistance of the gas layer becomes comparable to the combined thermal resistance of the wall and the condensate film. In the latter case, the net thermal resistance is given by a more complicated relation (55).

Furthermore, the condensate film thickness profile was derived from first principles using lubrication approximation. Self-consistency of the solution for mass transport across the gas and liquid layer and heat transport through the gas, liquid, and solid layer allowed us to obtain a solution that is different from that predicted by Nusselt's classical laminar condensation theory [1] which uses unrealistic assumptions. In particular, we have shown that the unavoidable thermocapillary stresses cannot be neglected and play an important role, notably changing the thickness profile, making it flatter. The effect of thermocapillary stresses is especially important at the very top of the cold wall, where the thickness of the condensate film remains finite (and as large as 50% of the maximal thickness at the bottom of the cold wall in the geometry considered here). As a result, no unphysical singularities (e.g., in the heat/mass flux) arise in the present description.

[1] W. Nusselt, "Die oberflachenkondensation des wasserdampfes," *Zeitschrift des Vereins Deutscher Ingenieure*, vol. 60, p. 569, 1916.

[2] D. F. Othmer, "The condensation of steam," *Ind. Eng. Chem.*, vol. 21, no. 6, pp. 576–583, 1929.

[3] H. Al-Diwany and J. Rose, "Free convection film condensation of steam in the presence of non-condensing gases," *International Journal of Heat and Mass Transfer*, vol. 16, no. 7, pp. 1359–1369, 1973.

[4] S. Park, M. Kim, and K. Yoo, "Condensation of pure steam and steam-air mixture with surface waves of condensate film on a vertical wall," *International Journal of Multiphase Flow*, vol. 22, no. 5, pp. 893–908, 1996.

[5] S. Al-Shammari, D. Webb, and P. Heggs, "Condensation of steam with and without the presence of non-condensable gases in a vertical tube," *Desalination*, vol. 169, no. 2, pp. 151–160, 2004.

[6] K.-Y. Lee and M. H. Kim, "Experimental and empirical study of steam condensation heat transfer with a noncondensable gas in a small-diameter vertical tube," *Nuclear Engineering and Design*, vol. 238, no. 1, pp. 207 – 216, 2008.

[7] J. Su, Z. Sun, G. Fan, and M. Ding, "Experimental study of the effect of non-condensable gases on steam condensation over a vertical tube external surface," *Nuclear Engineering and Design*, vol. 262, pp. 201–208, 2013.

[8] A. P. Colburn and O. A. Hougen, "Design of cooler condensers for mixtures of vapors with noncondensing gases," *Industrial & Engineering Chemistry*, vol. 26, no. 11, pp. 1178–1182, 1934.

[9] M. Saraireh, G. Thorpe, *et al.*, "Condensation of vapor in the presence of non-condensable gas in condensers," *International Journal of Heat and Mass Transfer*, vol. 54, no. 17-18, pp. 4078–4089, 2011.

[10] C. Chantana and S. Kumar, "Experimental and theoretical investigation of air-steam condensation in a vertical tube at low inlet steam fractions," *Applied Thermal Engineering*, vol. 54, no. 2, pp. 399–412, 2013.

[11] P. F. Peterson, V. E. Schrock, and T. Kageyama, "Diffusion layer theory for turbulent vapor condensation with noncondensable gases," *Journal of Heat Transfer-Transactions of the Asme*, vol. 115, no. 4, pp. 998–1003, 1993.

[12] T. Kageyama, P. F. Peterson, and V. E. Schrock, "Diffusion layer modeling for condensation in vertical tubes with noncondensable gases," *Nuclear Engineering and Design*, vol. 141, no. 1-2, pp. 289–302, 1993.

[13] C. Y. Warner and V. S. Arpaci, "An experimental investigation of turbulent natural convection in air at low pressure along a vertical heated flat plate," *International Journal of Heat and Mass Transfer*, vol. 11, no. 3, pp. 397–406, 1968.

[14] F. Blangetti, R. Krebs, and E. Schlunder, "Condensation in vertical tubes-experimental results and modeling," *Chemical Engineering Fundamentals*, vol. 1, no. 2, pp. 20–63, 1982.

[15] H. J. H. Brouwers, "Effect of fog formation on turbulent vapor condensation with noncondensable gases," *Journal of Heat Transfer-Transactions of the Asme*, vol. 118, no. 1, pp. 243–245, 1996.

[16] S. Oh and S. T. Revankar, "Experimental and theoretical investigation of film condensation with noncondensable gas," *International Journal of Heat and Mass Transfer*, vol. 49, no. 15-16, pp. 2523–2534, 2006.

[17] E. M. Sparrow and S. H. Lin, "Condensation heat transfer in the presence of a noncondensable gas," *Journal of Heat Transfer*, vol. 86, no. 3, pp. 430–436, 1964.

[18] W. Minkowycz and E. Sparrow, "Condensation heat transfer in the presence of noncondensables, interfacial resistance, superheating, variable properties, and diffusion," *Int. J. Heat Mass Trans.*, vol. 9, p. 1125, 1966.

[19] J. W. Rose, "Condensation of a vapour in presence of a non-condensing gas," *International Journal of Heat and Mass Transfer*, vol. 12, no. 2, p. 233, 1969.

[20] X. Wu, T. Li, Q. Li, and F. Chu, "Approximate equations for film condensation in the presence of non-condensable gases," *International Communications in Heat and Mass Transfer*, vol. 85, pp. 124–130, 2017.

[21] R. Savino and D. Paterna, "Marangoni effect and heat pipe dry-out," *Phys. Fluids*, vol. 18, p. 118103, 2006.

[22] R. W. Schrage, *A Theoretical Study of Interface Mass Transfer*. New York: Columbia University Press, 1953.

[23] T. Qin and R. O. Grigoriev, "The effect of noncondensables on buoyancy-thermocapillary convection of volatile fluids in confined geometries," *Int. J Heat Mass Transf.*, vol. 90, pp. 678–688, 2015.

[24] T. Qin, Ž. Tuković, and R. O. Grigoriev, "Buoyancy-thermocapillary convection of volatile fluids under atmospheric conditions," *Int. J Heat Mass Transf.*, vol. 75, pp. 284–301, 2014.

[25] T. Qin, Ž. Tuković, and R. O. Grigoriev, "Buoyancy-thermocapillary convection of volatile fluids under their vapors," *Int. J Heat Mass Transf.*, vol. 80, pp. 38–49, 2015.

[26] R. O. Grigoriev and T. Qin, "The effect of phase change on stability of convective flow in a layer of volatile liquid driven by a horizontal temperature gradient," *J. Fluid Mech.*, vol. 838, pp. 248–283, 2018.

[27] Y. Li, R. O. Grigoriev, and M. Yoda, "Experimental study of the effect of noncondensables on buoyancy-thermocapillary convection in a volatile low-viscosity silicone oil," *Phys. Fluids*, vol. 26, p. 122112, 2014.